

Adsorption of RB dye by Ce and Er Doped SnO₂ Photocatalysts for Water Remediation

Harita Kumari^a, Sonia^b, Sourabh Sharma^c, Parmod Kumar^d, Ashok Kumar^{b*} & Rajesh Parmar^a

^aDepartment of Physics, Maharshi Dayanand University, Rohtak, Haryana 124 001, India

^bDepartment of Physics, Deenbandhu Chhotu Ram University of Science and Technology, Murthal, Haryana 131 039, India

^cDepartment of Physics, Netaji Subhas University of Technology, New Dehli 110 078, India

^dDepartment of Physics, J. C. Bose University of Science and Technology, YMCA, Faridabad, Haryana 121 006, India

Received 7 July 2023; accepted 1 August 2023

This study focuses on synthesis of pure SnO₂ nanoparticles and SnO₂ nanoparticles doped with Erbium (Er) at 7% and Cerium (Ce) at 7% using sol-gel method. The aim was to evaluate their photocatalytic performance in degrading the harmful Rose bengal dye. XRD analysis confirmed that both undoped and rare earth-doped SnO₂ nanoparticles exhibited a tetragonal rutile structure. Photoluminescence (PL) analysis revealed an increase in oxygen vacancy concentration with higher dopant incorporation. Furthermore, band gap of doped SnO₂ nanoparticles was reduced compared to pure SnO₂. The reduction in the band gap was primarily attributed to creation of vacancy defects caused by dopants. Photocatalytic experiments demonstrated that within 60 minutes of UV light exposure, Er 7% doped SnO₂ nanoparticles achieved the degradation of 95.32% of Rose bengal dye. These findings highlight the potential of Er 7% doped SnO₂ as a highly effective catalyst for large-scale degradation of industrial waste, specifically organic dyes.

Keywords: Adsorption; Photocatalysis; Photoluminescence; Dye Degradation; Rare Earth

1 Introduction

The environmental changes caused by growing industrialization have been blamed for the continuous deterioration in human health¹. Due to their non-degradable nature, dyes are often resistant to degradation and can persist in water bodies for extended periods, leading to detrimental effects on aquatic ecosystems and human health². Taking into account these facts, researchers have been exploring the potential of oxide-based nanomaterials, such as CeO₂, SnO₂, ZnO, TiO₂, Mn₂O₃, and others, for various applications, including waste decomposition and remediation. SnO₂, or tin (IV) oxide, is a safe and eco-friendly metal oxide with unique properties, enabling it to serve as a useful photocatalyst in various applications³. However, photocatalytic performance of SnO₂ can be limited by certain factors, including its wide band gap and high recombination rate of photo generated electron-hole pairs. These limitations have led researchers to explore strategies in order to enhance the photocatalytic efficiency of SnO₂. Doping of rare-earth ions into SnO₂ can alter its band structure by

introducing new defect levels. This modification can result in a narrowed band gap and improved absorption of UV light⁴.

The current study focuses on the synthesis of SnO₂ nanoparticles using sol-gel technique and investigates photocatalytic potential of both pure SnO₂ nanoparticles and those doped with Erbium (Er) and Cerium (Ce) ions.

2 Materials and Methods

In the synthesis of Er-SnO₂ and Ce-SnO₂ nanoparticles, a stoichiometric amount of Erbium nitrate and Tin chloride was dissolved in an optimum amount of ethylene glycol. The solution was stirred at 120 °C until a gel formation, followed by drying at 200 °C to obtain powder. The powder was then annealed at 600 °C for 2 hours to produce nanoparticles. The same procedure was followed for the synthesis of Ce and Er doped SnO₂ nanoparticles (NPs). Structural analysis of the samples was conducted using a Rigaku X-Ray Diffractometer, and photoluminescence spectroscopy were recorded using a HORIBA FLUOROMAX Spectrofluorometer. Photocatalytic activity and band gap were investigated using a LABINDIA UV 3092 UV-VIS spectrophotometer.

*Corresponding author: (E-mail: ashokkumar.phy@dcrustm.org)

3 Results and Discussion

3.1 X-Ray Diffraction (XRD)

The XRD pattern of Er and Ce-doped SnO₂ samples (Fig. 1(a)) reveals diffraction peaks corresponding to a rutile tetragonal structure of SnO₂ (JCPDS card No. 41-1445). This indicates that the doped material is successfully incorporated into host lattice⁵. XRD analysis of the Er and Ce-doped SnO₂ samples reveal absence of additional impurity peaks associated with cerium or erbium oxide. This finding provides evidence that there is only one crystalline phase present in all the synthesized samples. The crystallite size of synthesized samples was determined using Debye-Scherrer's equation, as presented in Table 1.

3.2 Photoluminescence Spectroscopy (PL)

In order to learn more about defect concentration, the photoluminescence spectra of each sample was carried out with a 320 nm excitation wavelength at ambient temperature. The PL spectra of undoped

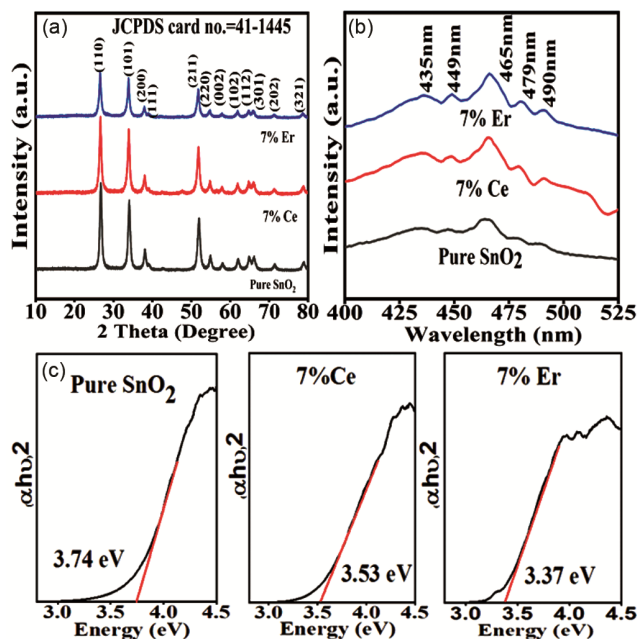


Fig. 1 — (a) XRD pattern, (b) PL spectra of pure, Er and Ce-doped SnO₂ samples, (c) Kubelka-Munk plots for bandgap determination of pure, Ce and Er-doped SnO₂ samples.

Table 1 — Structural and UV-Visible spectroscopic results of synthesized samples

Samples	Crystallite size (D)	Band Gap	Degradation efficiency	E _C (INR)
Pure SnO ₂	12.36 nm	3.74 eV	77.30%	2.20
7% Ce	11.71 nm	3.53 eV	90.68%	1.46
7% Er	11.68 nm	3.37 eV	95.32%	1.10

and doped SnO₂ nanoparticles are shown in Fig. 1(b), and they exhibit peaks at 435, 449, 465, 479 and 490 nm in wavelength. The oxygen vacancies and tin interstitials in SnO₂ lattice are responsible for these peak energy levels, which are linked to defects. The most often found defects in SnO₂ nanostructures are oxygen vacancies. In SnO₂ semiconductors, oxygen vacancies are known as “deep defect donors as they produce new donor “levels within the band gap⁶. Emission peaks in the 400-500 nm range are attributed to doubly ionized oxygen vacancies, indicating presence of shallow trapped states within band gap, comprising multiple subbands⁷. The amplification of visible emission peaks is commonly attributed to a higher concentration of defects, including oxygen vacancies, in SnO₂ lattice⁵.

3.3 UV-Visible Spectroscopy

The optical band gap (E_g) of synthesized nanoparticles was determined by utilizing UV-visible diffuse reflectance spectra and analyzing it through Kubelka-Munk function, represented by equation $F(R) = (1-R)^2/2R$ ⁸. By analyzing the results, it was observed that the band gap decreased from “3.74 eV for pure SnO₂ to 3.53 eV for 7% Ce and further to 3.37 eV for 7% Er, as depicted in Fig. 1(c). The reduction in the band gap can be attributed to an increase in defects resulting from the introduction of rare earth elements through doping, as indicated by photoluminescence spectra.

3.4 HRTEM Analysis

The investigation focused on morphological characteristics and particle size of both pure and doped SnO₂ samples using High-Resolution Transmission Electron Microscopy (HRTEM). Fig. 2 presents HRTEM images of synthesized pure SnO₂ and Ce- and Er-doped SnO₂ nanoparticles. The majority of particles exhibited spherical morphologies and showed no significant changes in Fig. 2(a,b,c). These results are consistent with X-ray diffraction (XRD) data, and the average particle sizes were determined to be approximately 15.27 nm for pure SnO₂, 13.75 nm for 7% Ce-doped SnO₂, and 12.12 nm for 7% Er-doped SnO₂ NPs.

3.5 Adsorption Behavior of Rose Bengal (RB) dye

The adsorption study of 7% Ce and 7% Er doped SnO₂ sample was conducted due to its superior photocatalytic properties in comparison to pure SnO₂.

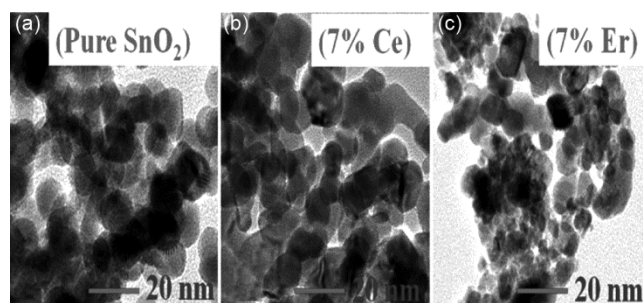


Fig. 2 — HRTEM images of (a) pure SnO₂, (b) 7% Ce and (c) 7% Er.

The study aimed to investigate and understand its adsorption behavior, which is crucial for its photocatalytic performance. The purpose of adsorption experiment was to determine how effectively an organic pollutant adsorbs to adsorbate; only one organic pollutant RB dye, was used to demonstrate this. The adsorption behavior of organic pollutants was measured by taking 0.4g/L of prepared nanoparticles, dispersed homogeneously into a 50 mL solution of RB dye (10ppm). When the mixture was vigorously stirred in dark on a magnetic stirrer, a homogenous solution was obtained. The solutions were collected at different time intervals (5, 10, 15, 20, 25, 30, 35 and 40 min) to study adsorption kinetics at 25°C. The adsorption amount of RB dye was calculated using following equation

$$Q_t = \frac{(C_0 - C_t)V}{W}$$

Where Q_t is adsorption capacity, C_0 and C_t (mg/L) are initial concentration and concentration after time t , respectively, V (L) is volume of RB solution, and W (g) is weight of adsorbent.

3.5.1 Adsorption Kinetics

A kinetic study was done to evaluate adsorption behavior of RB dye on the surface of a doped SnO₂ as a function of contact time. Adsorption kinetics plays a vital role in the photodegradation process and reflects maximum adsorption capacity of the adsorbent. Fig. 3 depicts that adsorbate's maximum adsorption rate on adsorbent's surface was very fast during the first 10 min and then became slower and reached equilibrium point. The rapid adsorption is due to availability of many active sites on the adsorbent surface along with strong electrostatic attraction. After some time span, the electrostatic repulsive force between adsorbent and adsorbate plays a key role and is analogous to the decrease the adsorption rate and finally reaches the equilibration point.

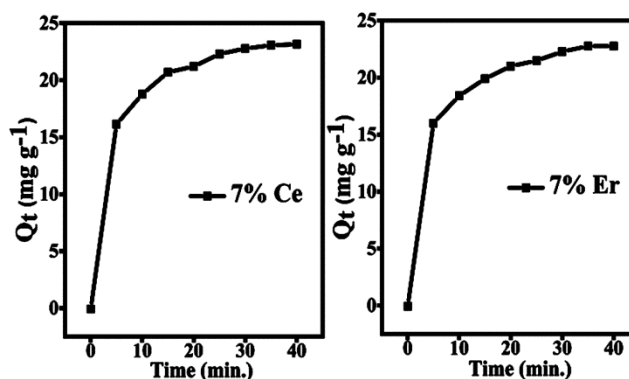


Fig. 3 — Contact time effect on the adsorption capacity of 7% Ce and 7% Er-doped SnO₂.

3.6 Photocatalytic Activity

To investigate the degradation of RB dye using Er and Ce-doped SnO₂ nanoparticles, a photocatalytic test was conducted. In this experiment, 0.02 gm of the produced catalyst was dispersed in a 50 ml solution of 10ppm RB dye to assess photocatalytic performance. After achieving adsorption-desorption equilibrium through 40 minutes of continuous stirring in dark, the suspension was exposed to UV radiation. The degradation rate of RB dye was monitored at regular intervals of 15 minutes using different photocatalysts, and the results are shown in Fig. 4. Degradation of RB dye was indicated by a gradual decrease in absorption peak intensity (Fig. 4(a-c)). The degradation efficiency increased from 77.30% for pure SnO₂ to 95.32% for 7% Er (Fig. 4(d)). The increase in degradation efficiency can be attributed to decrease in band gap and increase in oxygen vacancy defects, which facilitated faster electron transport from valence band (VB) to the conduction band (CB). The presence of 7% Er catalyst resulted in lowest remaining dye content (Fig. 4(e)), indicating a decreasing concentration of dye over time. Under UV light exposure, electrons transferred from VB to CB, generating holes. The interaction of these holes with OH group produced highly reactive hydroxyl radicals, while the interaction of electrons with oxygen molecules resulted in production of superoxide anions. These hydroxyl and superoxide radicals reacted with the dye, breaking it down into harmless substances such as CO₂ and H₂O.

Moreover, the photocatalytic degradation process closely adheres to first-order kinetics, as evidenced by linear relationship between $-\ln(C/C_0)$ and time, as shown in Fig. 2(f). This observation is further supported by R^2 values (Pure SnO₂=0.98, 7% Ce=0.95, 7% Er = 0.97), which are approximately

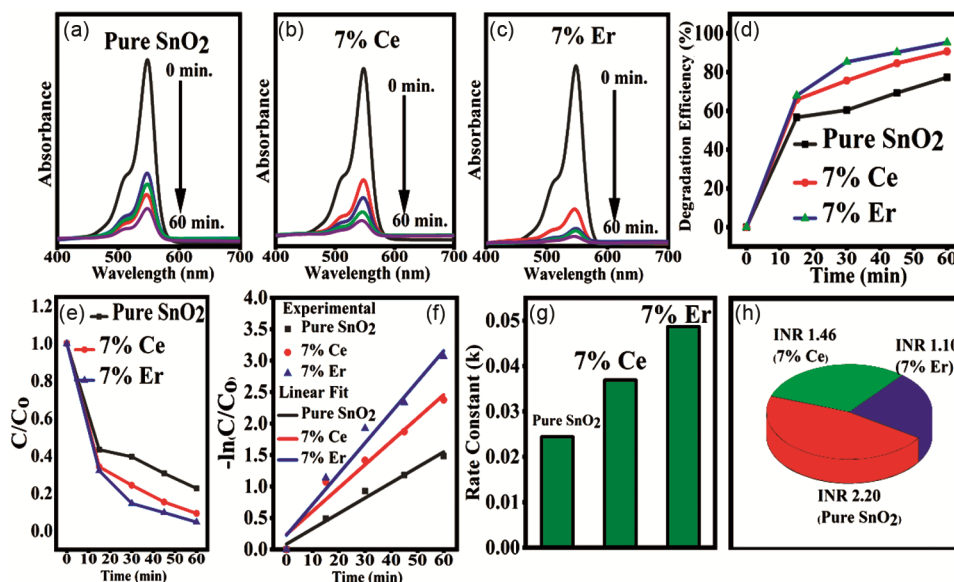


Fig. 4 — (a-c) Absorption spectra of dye at different time intervals, (d) % degradation with exposure time (e) C/C_0 versus degradation time, (f) linearly fitted curves of $-\ln(C/C_0)$ versus exposure time, (g) rate constant and (h) electricity cost by different photocatalysts.

equal to one⁹. The rate constant (k) is determined by fitting the curve between $-\ln(C/C_0)$ and time using linear regression. Fig. 4(g) demonstrates that the rate constant values increase with doping and reach their maximum in catalysts with a 7% Er concentration. In wastewater treatment, cost evaluation is a crucial aspect. Energy conservation, particularly in terms of electricity, is advantageous on a global scale. The electricity cost (E_c) for degradation of RB dye using the synthesized catalysts has been estimated. Notably, with 7% Er doping in SnO_2 matrix, the electricity cost is observed to be the lowest, coinciding with highest percentage of degradation, as shown in Fig. 4(h). Therefore, it can be observed that degradation of RB dye by these synthesized nanoparticles strongly depends on structural disorder or defects present.

4 Conclusion

Pure and Ce/Er-doped SnO_2 samples were synthesized via sol-gel technique to investigate their structural and optical behavior. From XRD analysis average crystallite size was found to be in the range 12.36-11.68 nm. PL analysis revealed a significant presence of oxygen vacancies. The Tauc plot indicated a decrease in optical band gap. Remarkably, the 7% Er-doped sample exhibited 95.32% degradation efficiency for RB dye, establishing it as the superior material for wastewater treatment.

Acknowledgement

Government of India through University Grant Commission (UGC-NTA) (Ref. No. 201610156900 & Roll No. HR05603954, dated- 04/02/2021) is acknowledged by the author for funding research fellowship and also, FIST Lab, Department of Physics, DCRUST, Murthal, for providing facilities for research.

References

- 1 Kumari H, Sonia, Chahal S, Suman, Kumar P, Kumar A & Parmar R, *Mater Sci Eng B*, 234 (2023) 116654.
- 2 Kumari H, Sonia, Suman, Ranga R, Chahal S, Devi S, Sharma S, Kumar S, Kumar P, Kumar S, Kumar A & Parmar R, *Water Air Soil Pollut*, 234 (2023) 349.
- 3 Bhawana, Kumar S, Sharma R, Gupta A, Tyagi A, Singh P, Kumar A & Kumar V, *New J Chem*, 46 (2022) 4014.
- 4 Sonia, Kumari H, Suman, Chahal S, Devi S, Kumar S, Kumar P & Kumar A, *Appl Phys A Mater Sci Proc*, 129 (2023) 91.
- 5 Singh G, Virpal & Singh R C, *Sens Actuators B Chem*, 282 (2019) 373.
- 6 Divya J, Pramothkumar A, Gnanamuthu S J, Victoria D C B & Prabakar P C J, *Phys B: Condens Matter*, 588 (2020) 412169.
- 7 Kumar V, Uma S & Nagarjan R, *Turk J Phys*, 38 (2014) 450.
- 8 Kumar V, Bhawna, Yadav S K, Gupta A, Dwivedi B, Kumar A, Singh P & Deori K, *Energy Environ Sci*, 4 (2019) 3722.
- 9 Chahal S, Rani N, Kumar A & Kumar P, *Vacuum*, 172 (2020) 109075.